



**HAL**  
open science

## The estimation of water erosion with **RUSLE** and deposition model: A case study of the Bin El-Ouidane dam catchment area (High Atlas, Morocco)

Wafae Nouaim, Dimitri Rambourg, Abderrazak El Harti, Ettaqy Abderrahim, Mohamed Merzouki, Ismail Karaoui

### ► To cite this version:

Wafae Nouaim, Dimitri Rambourg, Abderrazak El Harti, Ettaqy Abderrahim, Mohamed Merzouki, et al.. The estimation of water erosion with **RUSLE** and deposition model: A case study of the Bin El-Ouidane dam catchment area (High Atlas, Morocco). *Journal of Water and Land Development*, 2023, 58, pp.136-147. 10.24425/jwld.2023.146606 . hal-04887382

**HAL Id: hal-04887382**

<https://hal.science/hal-04887382v1>

Submitted on 14 Jan 2025








**HAL** is a multi-disciplinary open access archive for the deposit and dissemination of scientific research documents, whether they are published or not. The documents may come from teaching and research institutions in France or abroad, or from public or private research centers.

L'archive ouverte pluridisciplinaire **HAL**, est destinée au dépôt et à la diffusion de documents scientifiques de niveau recherche, publiés ou non, émanant des établissements d'enseignement et de recherche français ou étrangers, des laboratoires publics ou privés.



Distributed under a Creative Commons Attribution - NonCommercial - NoDerivatives 4.0 International License

# The estimation of water erosion with RUSLE and deposition model: A case study of the Bin El-Ouidane dam catchment area (High Atlas, Morocco)

Wafae Nouaim<sup>1)</sup>  , Dimitri Rambourg<sup>2)</sup> , Abderrazak El Harti<sup>1)</sup> ,  
 Ettaqy Abderrahim<sup>3)</sup> , Mohamed Merzouki<sup>1)</sup> , Ismail Karaoui<sup>1)</sup> 

<sup>1)</sup> University Sultan Moulay Slimane, Faculty of Sciences and Techniques, Team of Remote Sensing and GIS Applied to Geosciences and Environment, Av Med V, BP 591, Beni-Mellal 23000, Morocco

<sup>2)</sup> Université de Strasbourg, CNRS/EOST, ITES UMR 7063, Institut Terre et Environnement de Strasbourg, France

<sup>3)</sup> University Sultan Moulay Slimane, Faculty of Sciences and Techniques, Environmental, Ecological and Agro-industrial Engineering Laboratory, Beni-Mellal, Morocco

RECEIVED 25.02.2022

ACCEPTED 15.05.2023

AVAILABLE ONLINE 29.09.2023

**Abstract:** Water erosion is a critical issue for Morocco, especially in its semi-arid regions, where climatic and edaphic conditions only allow erratic soil formation and vegetation growth. Therefore, water erosion endangers human activity both directly (loss of arable land, landslides, mudflows) and indirectly (siltation of dams, river pollution).

This study is part of the Kingdom's effort to assess the risk of water erosion in its territory. It is dedicated to the Bin El-Ouidane dam water catchment, one of the biggest water storage facilities in the country, located in the High Atlas Mountains. The poorly developed soils are very sensitive to erosion in this mountainous area that combines steep slopes and sparse vegetation cover. The calculation of soil losses is carried out with the RUSLE model and corrected by estimating areas of deposition based on the unit stream power theory. This method produces a mean erosion rate of around  $6.3 \text{ t}\cdot\text{ha}^{-1}\cdot\text{y}^{-1}$ , or an overall annual loss of 4.1 mln t, consistently with the siltation rate of the dam. Primary risk areas (erosion rates  $> 40 \text{ t}\cdot\text{ha}^{-1}\cdot\text{y}^{-1}$ ) account for 54% of the total losses, while they cover only 7% of the catchment. This distribution of the soil losses also shows that the erosion risk is mainly correlated to slope, directing the means of control toward mechanical interventions.

**Keywords:** remote sensing, RUSLE, unit stream power theory, water erosion

## INTRODUCTION

Water erosion is one of the main forms of soil degradation. The term refers to all detachment, transport, and sedimentation processes occurring on the soil surface at different spatial and temporal scales (Le Bissonnais *et al.*, 1998; Julien, 2010). The main factors influencing erosion are rainfall, pedology, topography, land use, and cultivation practices in an agricultural context.

For the past 30 years, Morocco has been experiencing the most severe drought episode in its contemporary history. In this region, particularly in the High Atlas Mountains, the growth of vegetation cover is limited by this aggravating water deficit. This

situation results in ecosystems vulnerable to soil degradation through water erosion (MAEF, 2013). According to the FAO (2015), 40% of land in Morocco is affected by the phenomenon, including 125,000 km<sup>2</sup> of cropland and rangeland (Maimouni *et al.*, 2011). It is assumed that the degradation exceeds  $20 \text{ t}\cdot\text{ha}^{-1}\cdot\text{y}^{-1}$  in slopes of the Rif and lies between 5 and  $10 \text{ t}\cdot\text{ha}^{-1}\cdot\text{y}^{-1}$  in the Middle and High Atlas, threatening the sustainability of agriculture.

Another drawback is that large dams in Morocco receive about 50 mln t of sediment per year, which reduces their water storage capacity by about 0.5% annually (Merzouki, 1992; Badraoui and Hajji, 2001). This siltation has negative effects on

the production of electricity and the supply of drinking and irrigation water (loss of a volume corresponding to the irrigation of 10,000 ha·y<sup>-1</sup>).

In the context of the national effort to characterise and combat erosion, the present study focuses on the Bin El-Ouidane dam catchment area, located in the High Atlas Mountains. The erosion risk has been estimated using the RUSLE (Revised Universal Soil Loss Equation) model (Renard *et al.*, 1997). Part of its input parameters are characterised using remote sensing techniques and adapted for the high-mountain regional context (steep slopes, snow cover). The model allows both the quantitative estimation of the phenomenon and the spatial distribution of losses to guide prevention programs. However, it does not take into account a central aspect of the soil and sediment cycle: deposition. Therefore, this study corrects the results produced by RUSLE via estimation of deposition areas according to the unit stream power theory (Moore and Burch, 1986).

## MATERIAL AND METHODS

### DESCRIPTION OF THE BIN EL-OUIDANE DAM CATCHMENT AREA

#### Localisation and geomorphology

The Bin El-Ouidane dam is located in the central Moroccan High Atlas, 54 km southwest of the city of Beni Mellal and 27 km northeast of the town of Azilal (Fig. 1). Built in 1953 over 3,800 ha for multiple purposes (drinking water supply, irrigation of the Beni Moussa perimeter, electricity production, tourism, sport, and leisure), it initially stored around 1,500 mln m<sup>3</sup>. The dam is located at the confluence of two rivers, the El-Abid River and

Assif Ahansal, and its catchment. It thus covers an area of 6,480 km<sup>2</sup>.

The El-Abid River has its source in Jbel Masker at an altitude of 3,277 m. Its daily average flow rate reaches 6.58 m<sup>3</sup>·s<sup>-1</sup> before the confluence, that is, a contribution of 207.5 mln m<sup>3</sup> per year. As it continues its course downstream from the dam, it is the main tributary of the Oum Er-Rbia River and a major supplier for the Tadla plain aquifer.

The average throughput of the Ahansal River is 9.41 m<sup>3</sup>·s<sup>-1</sup>, or 296.8 mln m<sup>3</sup> per year, draining almost half of the catchment area.

The transport of sediment through its tributaries causes silting of the dam with about 5 mln m<sup>3</sup>·y<sup>-1</sup> [Badraoui and Hajji, 2001]. Recent data from the High Commission for Water, Forests, and the Fight against Desertification (unpublished) show that the dam has lost 17% of its capacity in 50 years, mainly because of water erosion.

The geographical position of the Bin El-Ouidane dam catchment area, straddling the Middle and High Atlas, gives it very steep reliefs. The topography of the study area presents a strong altitudinal gradient (more than 1,500 m difference in altitude), from south and southeast (upstream) to north and northwest (downstream). The relief can be subdivided into three groups: mountains, plateaus, and depressions (or valleys) (Fig. 2).

The mountainous areas correspond to the higher altitudes in the south and southeast of the catchment area. They occupy about 46% of the total area. The main peaks are Jbel Azourki (3,677 m), Jbel Mourik (3,300 m), and Jbel Issoual (2,800 m).

The plateaus correspond to areas of intermediate altitude. They are well distributed over the catchment, with the exception of its northeast part, and they represent about 28% of the total area. The Ait Abdi plateau extends south of the catchment area with altitude between 2,200 and 3,000 m. Towards the east of the

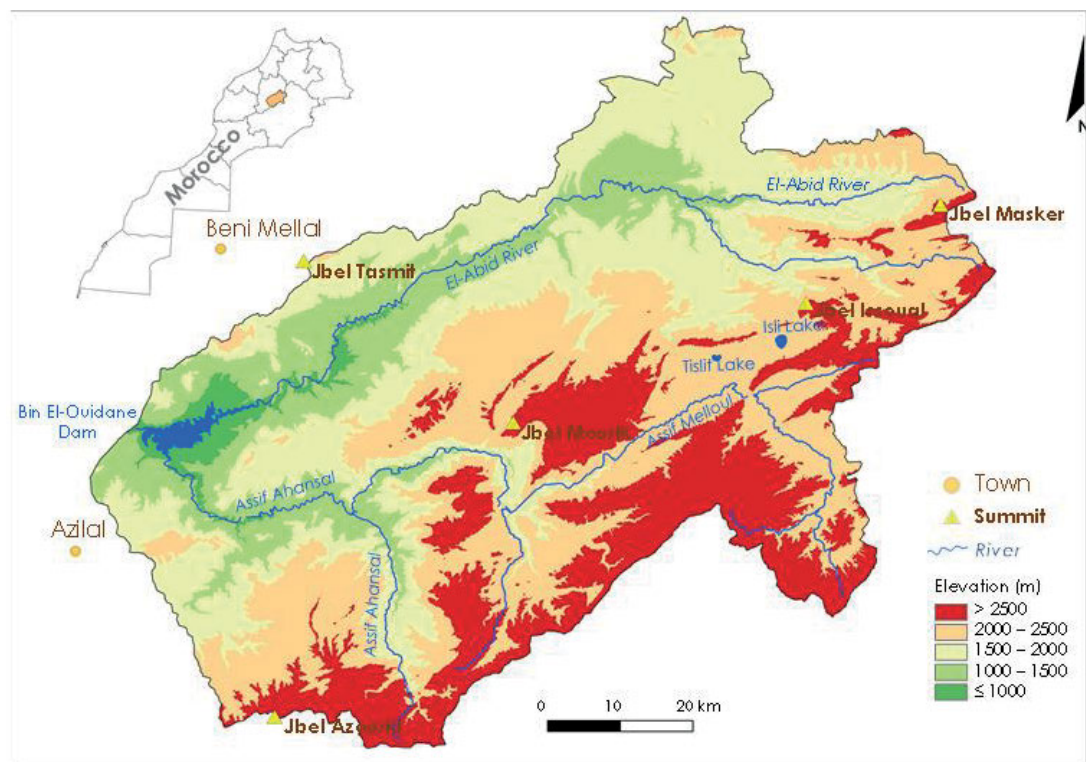


Fig. 1. Location and topography of the Bin El-Ouidane dam's catchment area; source: own elaboration

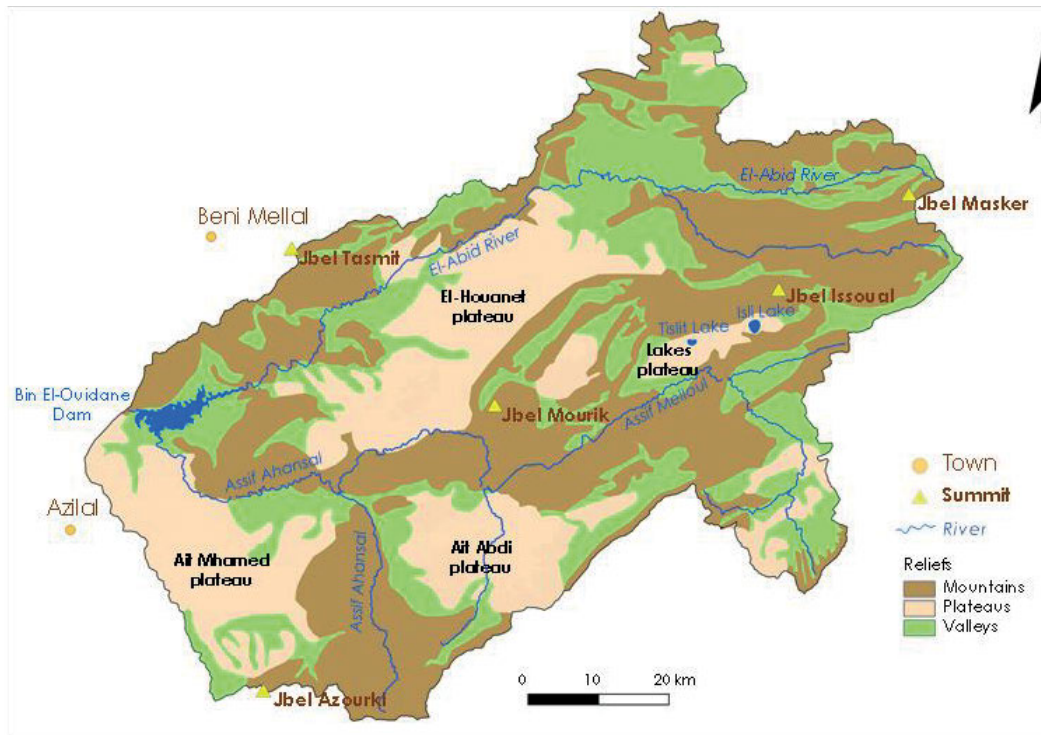


Fig. 2. Reliefs classification of the Bin El-Ouidane dam catchment area; source: own elaboration

watershed located are the Isly and Tislit lake plateaus dominated by the Jbel Bab n'Ouaya. Towards the west of the watershed, the Ait Mhmed plateau is a flat-bottomed syncline dominated by Dogger limestone. It extends over 1,700–2,600 m in altitude and is bounded to the east by the Assif Ahansal River and its tributary Assif Wabzaza.

The valleys and depressions correspond to lower elevations. They represent about 26% of the total area of the study zone. They mainly run along the watercourses and sometimes take the

form of large valleys, punctually occupied by irrigated or dry crops as well as a few scattered urbanised areas. The main valleys are El-Abid, Assif Ahansal, and Assif Melloul.

**Climate (rainfall and temperature)**

Meteorological stations installed in the catchment area of the Bin El-Ouidane dam or its immediate vicinity show an irregular distribution (Fig. 3). Indeed, these stations are located at low altitudes, between 1,000 and 2,000 m, mainly along the El-Abid

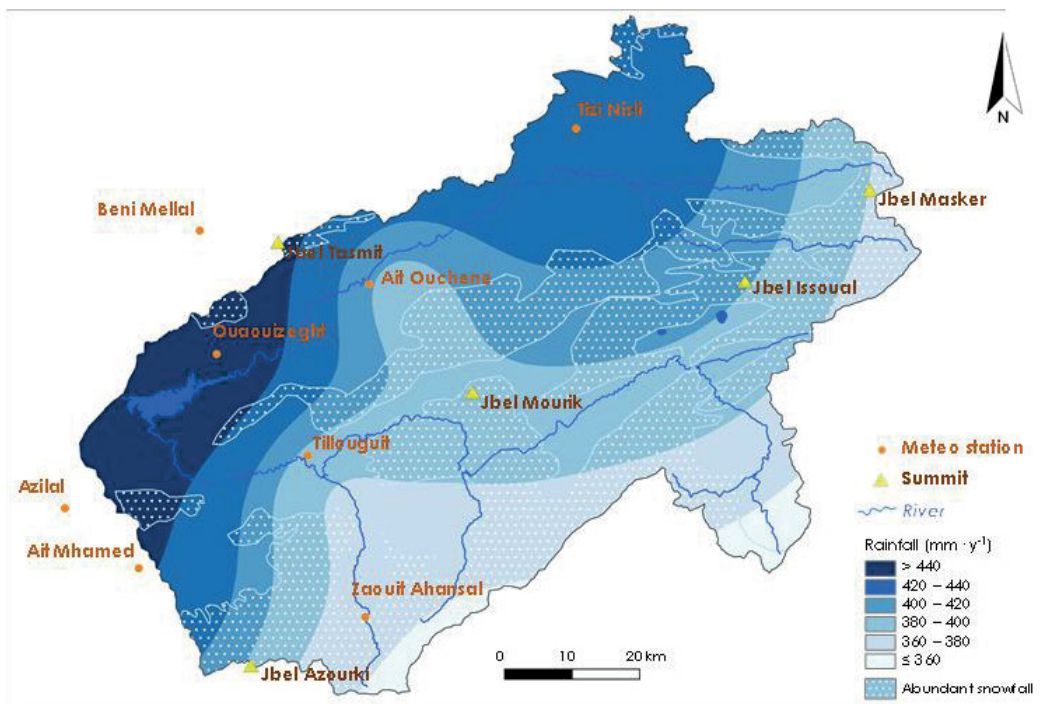


Fig. 3. Rainfall distribution over the Bin El-Ouidane dam catchment area; source: own elaboration

River and the Assif Ahansal River. Above 2,000 m, no stations are installed due to the lack of road infrastructure and unfavorable weather conditions.

The spatial distribution of rainfall shows moderate heterogeneity, with a difference between the maximum and minimum annual rainfall of about 100 mm. The low-lying areas (below 1,500 m) are the wettest. They receive 400 mm or more of rainfall annually, while the high-altitude areas (above 1,500 m) receive between 346 and 400 mm. The decreasing rainfall gradient along the northwest-south axis is possibly exaggerated due to the absence of high-altitude stations, resulting in an extrapolation artifact. Incidentally, this result is consistent with the fact that above 2,000 m altitude, precipitation often comes as snow (Fig. 3). At altitudes of 3,500 m and above, the snow cover can last for more than two months in a normal year. Regarding erosion, snowfall does not have the same characteristics as rain (almost zero kinetic energy), so this uncertainty in the data does not produce any conceptual incompatibility with the modeled phenomenon.

The intra-annual variability of rainfall is quite significant. This variability has a direct influence on the flows in the rivers in the area, with low water levels and even very marked and long-lasting droughts during the summer season. Indeed, rainfall mainly occurs from September to May, with winter maxima between November and January and spring maxima in March and April. During summer, rainfall only appears in the form of sudden convective storms. These characteristics are typical of the semi-arid climate. In summary, the study area experiences two seasons during the year: a dry season that lasts six months, from May to October, and a wet season that lasts from November to April.

Like rainfall, temperatures in the catchment area are subject to the altitudinal gradient and seasonal variations. Annual averages vary between 12 and 19°C. Winter temperatures are

very low and can reach  $-9^{\circ}\text{C}$  during December and January, while summer maxima are around  $43^{\circ}\text{C}$  during July and August.

Up to 1,500 m altitude, the average annual temperatures are between 15 and  $18^{\circ}\text{C}$ . At higher altitudes, the temperature drops below  $12^{\circ}\text{C}$ , and recurrent frosts occur. Thus, the catchment area of the Bin El-Ouidane dam extends over different bioclimatic stages. In Azilal and Tillouguit, the bioclimate is semi-arid, whereas it becomes sub-humid higher up (e.g., Ait Mhamed).

### Geo(hydro)logy and pedology

The Central High Atlas is characterised by a significant geological diversity (Fig. 4). It contains geomorphological structures dating from the Triassic to the Cretaceous, and it has heterogeneous hydrodynamic characteristics (porosity, permeability) and particular structures (karstic plateaus).

The heterogeneity of lithological and relief formations gives the catchment area a singular hydrological and hydrogeological behaviour. The substratum of the catchment area is essentially made up of carbonate rocks (51% of the total surface), including limestones and dolomites from the Lias and the Dogger Sea. These permeable carbonate rocks (locally karstic) make the catchment area a considerable reservoir of groundwater. Conversely, the areas made up of impermeable sedimentary rocks (marl, clay, etc.) and the outcrops of magmatic rocks (gabbro and basalts) have a very low infiltration capacity.

From a pedological point of view, the catchment area is dominated by skeletal soils with low infiltration capacity and low water storage capacity (Aboulabbes, 2004). That includes raw or poorly developed mineral soils, due to the steepness of slopes, but also calcimagnesian soils that are rich in fine silicate particles. Locally and in very small proportions in the immediate vicinity of the hydrographic network, soils can show hydromorphic characteristics.

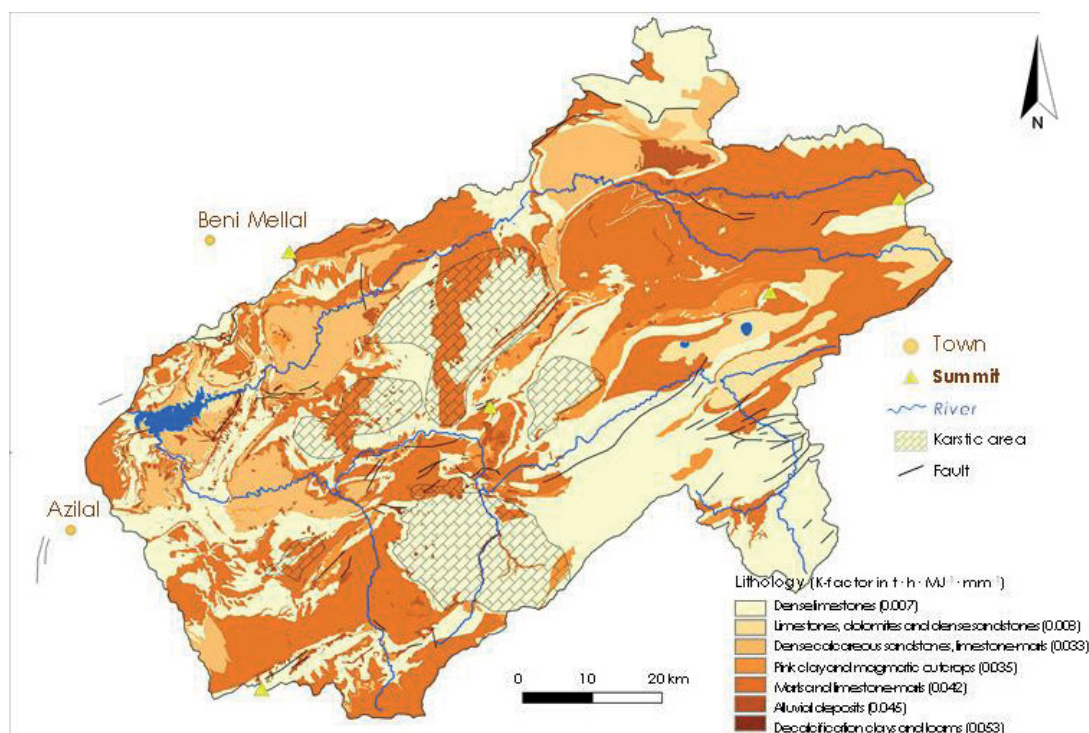


**Fig. 4.** Lithology and corresponding soil erodibility in the Bin El-Ouidane dam catchment area

### Land use

Due to climatic conditions on some slopes (temperature, sunshine, rainfall) and particular edaphic conditions (poor soils), the majority of the catchment area is characterised by bare soils or very sparse vegetation. However, part of the area is covered by forests (Fig. 5).

Thus, the downstream part of the catchment area is more covered than the upstream part, as most of the forest stands are located in thalwegs and along watercourses. The main species are Berber cedar, juniper, Aleppo pine, Atlas cedar, and Holm oak. Their distribution is influenced by altitude, slope exposure, edaphic conditions, and marginally by anthropic activities (overgrazing, logging). In this respect, the study site contains dense, medium-dense, and very sparse stands.

In contrast, the upstream part of the catchment area is generally devoid of any cover. As much as 46% of the land in the study area is almost desert-like due to very high altitudes (above 2,600 m) and it has climate characterised by very low temperatures and heavy snowfalls. At altitudes of 3,500 m and above, snow cover can last several months in a normal year. Although considered bare in terms of vegetation, these areas benefit from the protection of soil by the snow cover.

The human presence is very scattered in the study area. Agricultural activity is limited to fruit growing (olive trees) and some market gardening and fodder crops produced locally along the rivers. Higher up, certain areas are subject to extensive pastoral activity, the extent of which is difficult to characterise but it has an impact on the soil (overgrazing).

### REVISED UNIVERSAL SOIL LOSS EQUATION

The RUSLE (Revised Universal Soil Loss Equation) empirical model by Renard *et al.* (1997) is a further development of the USLE (Universal Soil Loss Equation) model by Wischmeier and Smith (1978). It was originally intended for the estimation of

water erosion at the scale of agricultural plots. This revision extended the scope of calculations to larger catchments with different land-use types. The spatial estimation approach of RUSLE is used in many studies to quantify the average annual soil losses due to water erosion, including in Mediterranean or semi-arid areas (Al Zitawi, 2006; Kouli, Soupios and Vallianatos, 2008; Khemiri and Jebari, 2021). In line with the Kingdom's erosion control program, the model is also preferred for studies in Morocco (Meliho *et al.*, 2016; Hara *et al.*, 2020; Manaouch, Zouagui and Fenjiro, 2021).

The model (Eq. 1) incorporates five factors, each representing a physical characteristic affecting the potential amount of soil eroded: rainfall kinetic energy, soil erodibility, topography, vegetation cover, and erosion control practices.

$$A = R \cdot K \cdot LS \cdot C \cdot P \quad (1)$$

where:  $A$  = soil loss ( $t \cdot ha^{-1} \cdot y^{-1}$ ),  $R$  = rainfall erosivity ( $MJ \cdot mm \cdot ha^{-1} \cdot h^{-1} \cdot y^{-1}$ ),  $K$  = soil erodibility ( $t \cdot h \cdot MJ^{-1} \cdot mm^{-1}$ ),  $LS$  = slope factor (-),  $C$  = land use (-);  $P$  = support practices (-).

### Rainfall erosivity (R-factor)

Precipitation is the main vector of water erosion. According to the formula of Wischmeier and Smith (1978), the erosivity of rainfall requires to estimate the kinetic energy and the average intensity over 30 minutes of each rain event.

In the present case study, these parameters are unavailable. Thus, it impossible to calculate the  $R$ -factor according to the method described initially in RUSLE. To remedy this, Arnoldus (1980) developed a substitution method based on annual and monthly rainfall amounts (Eq. 2).

$$R = \sum_{i=1}^{12} 1.735 \cdot 10^{1.5 \log \left( \frac{p_i^2}{P} \right) - 0.8188} \quad (2)$$

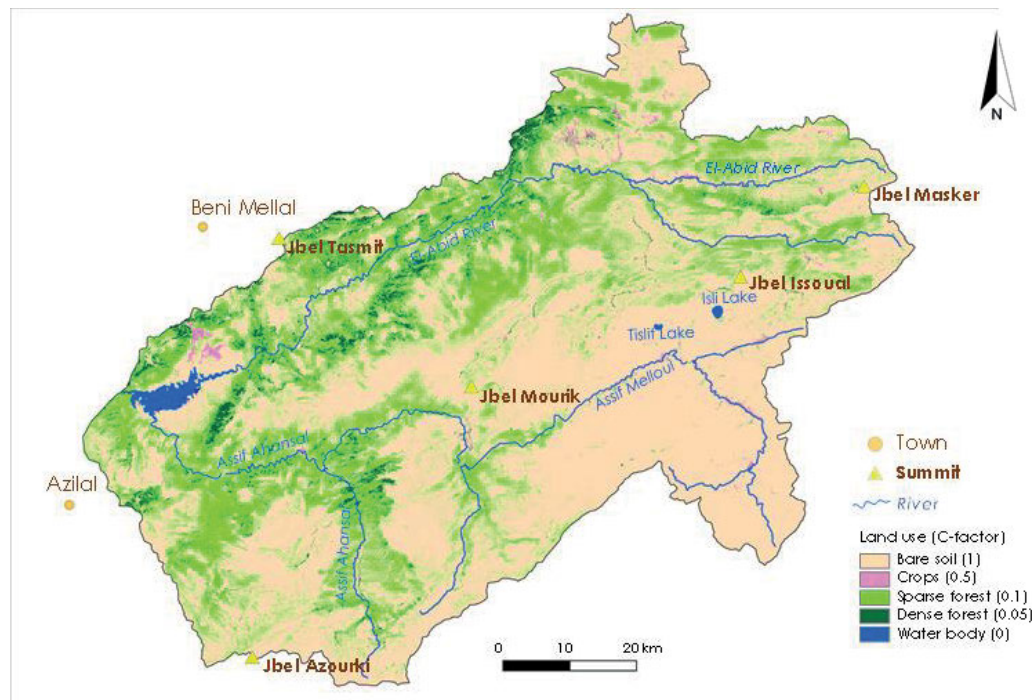


Fig. 5. Land cover and corresponding factor value in the Bin El-Ouidane dam catchment area; source: own elaboration

where:  $R$  = rainfall erosivity ( $\text{MJ}\cdot\text{mm}\cdot\text{ha}^{-1}\cdot\text{h}^{-1}\cdot\text{y}^{-1}$ ),  $P_i$  = average monthly rainfall (mm),  $P$  = average yearly rainfall (mm).

The data from the weather stations distributed over the catchment area (Fig. 3) are given by the Oum Er-Rbia water basin agency. The data cover an observation period of 34 years (1983–2017). Once calculated at the scale of each station, the rainfall erosivity values are interpolated using a deterministic method (multilevel B-spline acc. to Lee, Wolberg and Shin (1997)).

### Soil erodibility (K-factor)

Soil erodibility is a measure of the vulnerability of particles to be detached and transported by rain and runoff. Texture is the main factor influencing the  $K$ -factor, but soil structure, organic matter content, and permeability are also important (Stone and Hilborn, 2000). Hence, the formula proposed by Wischmeier, Smith and Umland (1958) takes these parameters into account. But the database of the parameters necessary to calculate the  $K$ -factor does not exist for the Bin El-Ouidane dam catchment area. Nevertheless, it was determined thanks to the regional geological map (scale of 1:50,000) and by associating an erodibility value according to the friability of each soil's parent rock (Tab. 1).

**Table 1.**  $K$ -factor and parent rock friability

Parent rock	$K$ -factor ( $\text{t}\cdot\text{h}\cdot\text{MJ}^{-1}\cdot\text{mm}^{-1}$ )	References
Dense limestones	0.007	Heusch (1970)
Limestones, dolomites and dense sandstones	0.008	Diallo (2000)
Dense calcareous sandstones and limestone-marls	0.033	Naslhaj (2009)
Pink clays and magmatic outcrops	0.035	Naslhaj (2009)
Marls and limestone-marls	0.042	Naslhaj (2009)
Alluvial deposits (terraces)	0.045	Naslhaj (2009)
Decalcification clays and loams	0.053	Heusch (1970)

Source: own elaboration based on literature.

### Slope length and steepness (LS-factor)

The topographic factor ( $LS$ -factor) represents the combined effect of slope steepness and slope length. Indeed, the slope affects the ability of runoff to detach and transport soil particles. The steeper the slope, the more kinetic energy the runoff acquires and the more it erodes the soil. The longer the slope, the greater the soil loss. Moreover, a long slope allows for more concentration of runoff flows, thus increasing the erosive potential.

For the Bin El-Ouidane dam catchment area, the formula retained for the  $LS$ -factor (Eq. 3) is adapted from Liu *et al.* (2000) and Liu, Zhang and Yun (2002), one of the only teams that has recalibrated this parameter for steep slopes, well beyond the initial application range of RUSLE. The slope length is calculated through a GIS procedure, following the methodology proposed by Mitasova *et al.* (1996), with a flow length limited to 300 m, in agreement with Winchell *et al.* (2008). This approach, akin to Schmidt, Tresch and Meusburger (2019), proves to be necessary

not to dramatically overestimate this factor in high-mountain contexts.

$$LS = \left(\frac{A}{22.13}\right)^{0.4} + a \sin\theta + b \quad (3)$$

where:  $LS$  = slope length and steepness factor (-);  $A$  = upslope contributing area per contour width ( $\text{m}^2\cdot\text{m}^{-1}$ );  $\theta$  = slope angle (rad);  $a = 10.8$  and  $b = 0.03$  if  $\theta \leq 5^\circ$ ,  $a = 16.8$  and  $b = 0.5$  if  $10 > \theta > 5^\circ$ ,  $a = 21.9$  and  $b = 0.96$  if  $\theta \geq 10^\circ$ .

The digital terrain model (DTM) used in this study belongs to the ASTER program (Advanced Spaceborne Thermal Emission and Reflection Radiometer) co-produced by MIT and NASA (with 30 m resolution).

### Land use (C-factor)

The land cover factor is a ratio of erosion on bare soil and under vegetation cover. It is often the main protective factor which helps to intervene to reduce erosion risks.

Indeed, the vegetation cover protects the soil by intercepting the raindrops, thanks to the aerial parts of the plants, allowing the dissipation of the kinetic energy and thus the reduction of the splash effect (Geddes and Dunkerley, 1999). It also slows down the formation of capping and, even more, preventing the formation of a sedimentary crust, the most advanced type of agricultural soil degradation. Thus, a high infiltration capacity is maintained, limiting the risk of runoff even during heavy rainfall (Ludwig, 2000). In the event of a runoff, stems and leaves form a screen against the path of water streams. Finally, the vegetation cover also helps to retain soil by root systems: plants improve the cohesion of soils and thus strengthen their mechanical properties (O'Loughlin and Zhang, 1986).

The  $C$ -factor of the study area was assessed by processing Sentinel-2 (MSI) satellite images produced by the European Space Agency in the framework of the Copernicus Earth observation program. Sentinel-2 images are composed of 13 spectral bands ranging from visible to mid-infrared.

The images used in this study are from July 27, 2021, and have a resolution of 10 m. The images required a correction for atmospheric anomalies. Indeed, the luminances recorded by the satellite sensor correspond to a complex signal resulting from the contribution of the earth surface and the atmosphere. Scattering can attenuate some of the energy illuminating the earth and the atmosphere, thus reducing the strength of the signal propagating from the target to the sensor.

Values of the  $C$ -factor depend mainly on the nature and percentage of vegetation cover. Therefore, the normalised vegetation index  $NDVI$  (Eq. 4) estimates and differentiates the different land uses.

$$NDVI = \frac{NIR - R}{NIR + R} \quad (4)$$

where:  $NDVI$  = normalised difference vegetation index,  $NIR$  = infrared spectral band,  $R$  = red spectral band.

The different land uses mapped (Fig. 5) are associated with a  $C$ -factor value (Tab. 2) based on the classification by Wischmeier and Smith (1978).

Dense forest offers the strongest protection: the interception of rain by the aerial parts of trees drastically reduces the kinetic

**Table 2.** Land use and *C*-factor association

Land use	<i>C</i> -factor
Crops	0.5
Dense forest	0.05
Sparse forest	0.1
Bare soils	1
Water	0

Source: own elaboration.

energy of rain and, therefore, the splash effect. Secondly, the trunks and any litter on the ground limit or even prevent the runoff phenomenon. Crops provide intermediate protection compared to bare soil, mainly due to their seasonality (growth and harvest phase).

#### Support practices (*P*-factor)

Anti-erosion practices are integrated into RUSLE as a semi-quantitative corrective factor (i.e. *C*-factor) representing soil conservation cultivation techniques. Indeed, certain cultural practices reduce the quantity and speed of runoff and, therefore, the erosive potential. The most used conservation practices are reverse slope tillage, contour plowing and ridging, and strip cropping (Roose and Bertrand, 1971). A value of 1 reflects the absence of support practice, whereas 0.1 is associated with the most protective techniques (e.g. partitioned ridging on a low slope) (Wischmeier, Smith and Uhland, 1958; Roose, 1973; Millington and Townshend, 1984).

Very little information is available on erosion control practices in the study area. The main actions implemented include reforestation, impact of which is already covered the definition of the *C*-factor, and some mechanical control campaigns (earthworks, hydraulic thresholds, grassy strips).

Methods based on satellite images can be used to locate and characterise certain erosion control practices (dry stone or gabion thresholds). But in the case of our study area, agricultural facilities (such as urban infrastructure) are combined with local resources (earth, gravel, pebbles). Thus, their surface characteristics do not differ sufficiently from the surrounding environment to distinguish them through remote sensing techniques.

In view of the lack of data and the small area covered by the anti-erosion intervention campaigns, the *P*-factor of the RUSLE model has been set at 1 for the entire catchment area.

#### Unit stream power theory based deposition model

The erosion depends on the slope angle and length as well as its profile (convexity/concavity) (Gray, 1971). This aspect is covered by the unit stream power theory (Moore and Burch, 1986), which aims at locating the areas of deposition and erosion by analysing the gradient of the erosive potential of flows along the slopes. In this study, we applied the continuous approach proposed by Mitasova *et al.* (1996), where the sediment transport capacity is calculated as derivative of the *LS*-factor (Eq. 5).

$$E = \frac{\partial LS}{\partial x} \cos \alpha + \frac{\partial LS}{\partial y} \sin \alpha \quad (5)$$

where: *E* = sediment transport capacity,  $\alpha$  = aspect angle (rad), *x* = coordinate on the W–E direction (m), *y* = coordinate on the N–S direction (m).

Negative values of the sediment transport capacity represent an erosive potential when positive values characterize a deposition area. Therefore, we excluded these areas from the computation of RUSLE and corrected the total soil loss calculation according to the global deposition potential.

## RESULTS AND DISCUSSION

### RAINFALL ERODIVITY FACTOR (*R*-FACTOR)

Interpolation of the calculated *R*-factor values for each meteorological station produces a rainfall erosivity map (Fig. 6).

Rainfall erosivity values range from 73 to 277 MJ·mm·ha<sup>-1</sup>·h<sup>-1</sup>·y<sup>-1</sup>. The highest values are located downstream of the catchment area. As the altitude rises, these values gradually decrease until reaching their lowest values at high peaks. On the one hand, this spatial distribution follows a rainfall gradient determined by the continental climate and, on the other hand, it follows a northwest-southeast altitudinal gradient.

In the high mountains, snow precipitation cannot be neglected in the calculation of the *R*-factor, as snowfall can occur over months. Indeed, this type of precipitation does not carry erosive energy in the same way as rain: snow falls in the form of crystals that float for a long time in the air before gently reaching the ground without damaging its surface structure. When computing the RUSLE equation, a correction was made to integrate this aspect into the calculation. In the zones concerned by heavy and durable snowfall, the rain erosivity factor was corrected by subtracting a third of its value (considering snowfall over four months on average).

Additionally, the melting of the snow cover also produces kinetic energy via the runoff it causes. However, in the absence of data on the dynamics and extent of this phenomenon, it is not included in the present work.

### SOIL ERODIBILITY (*K*-FACTOR)

The *K*-factor distribution in the Bin El-Ouidane dam catchment area is shown in Figure 4.

Most of the soils in the catchment area are not very developed. However, they can be divided into two categories according to the type of parent rock.

Approximately half of the catchment area has soils derived from calcareous marls, clays, or alluvial parent rock. Marls and clays are characterised by rapid mechanical weathering, a result of the hydration phenomenon leading to the formation of a loose mass of carbonated clay. Their limestone content varies from 15 to 30% (Pajot, 1963), so their ionic exchange capacity is often reduced, implying a low structural stability. Therefore, these facies are the most erodible, with values above 0.035 t·h·MJ<sup>-1</sup>·mm<sup>-1</sup>.

The rest of the soils, classified as moderately to slightly erodible, derive from coherent rocks (dense limestone, dolomites) characterised by low susceptibility to erosion. These facies are characteristic of the plateaus in the study area and its south-southeastern portion. Thus, they are associated with erodibility values of less than 0.035 t·h·MJ<sup>-1</sup>·mm<sup>-1</sup>.



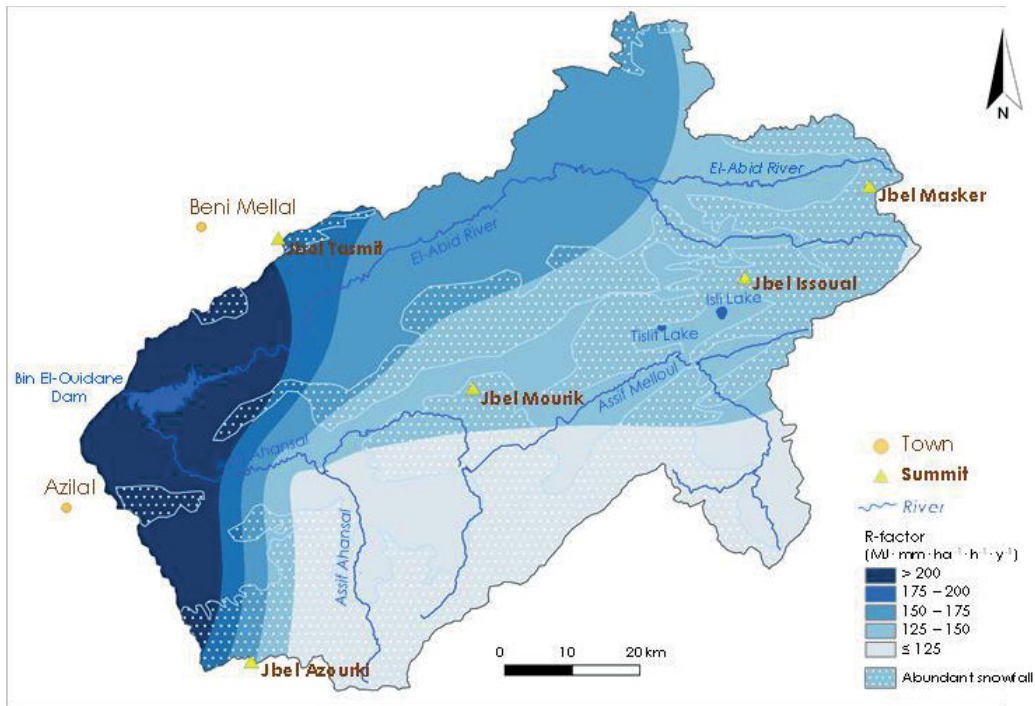


Fig. 6. Rainfall erosivity in the Bin El-Ouidane dam catchment area; source: own elaboration

Regarding the characteristics of the soils in the region, the land degradation process is subject to a negative feedback loop. Indeed, carbonate soils, losing their clay fraction, as the process progresses, become even more sensitive to water erosion. Thus, we often observe that erosion, initially occurring in sheet erosion, evolves in spectacular gullies.

In addition, certain mechanical phenomena create temporal fluctuation in soil erodibility: daily temperature cycle, seasonal freezing and thawing, and variation in soil water content. However,

the resolution of the data available and the very structure of the RUSLE model do not allow this level of refinement.

#### TOPOGRAPHY (LS-FACTOR)

Figure 7 maps the spatial distribution of the topographic factor (*LS*) in the study area.

Its values vary between 0 (flat area) and 55 (steep slope with a large upslope contributing area). The highest values are found

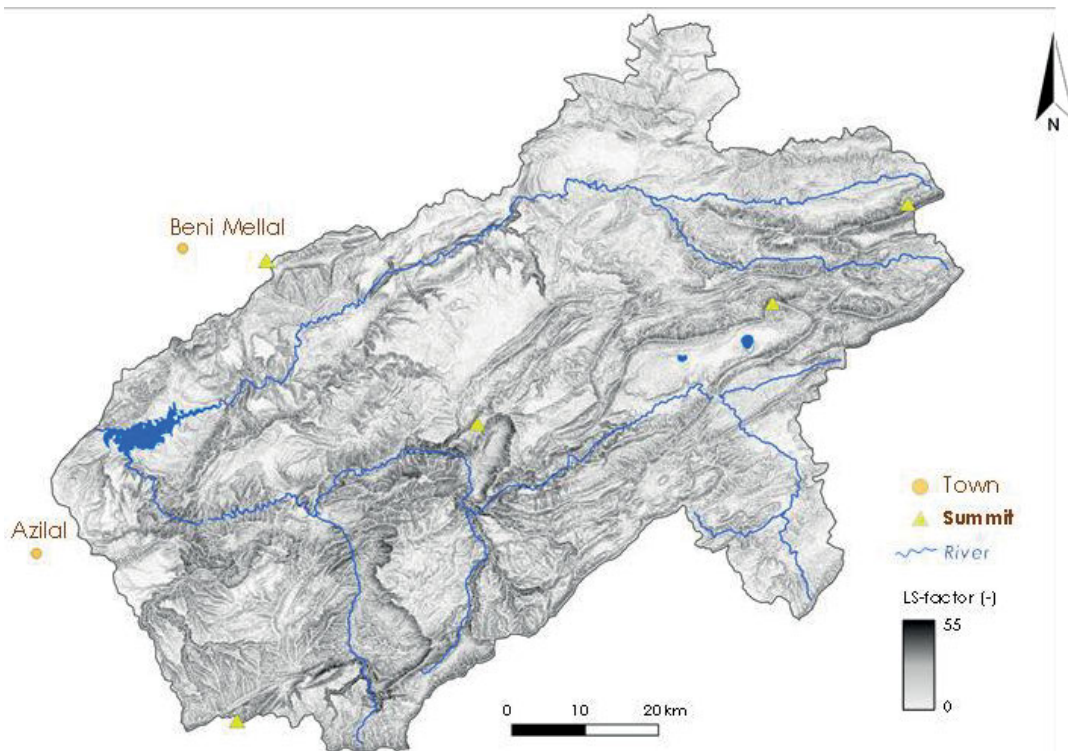


Fig. 7. Slope factor in the Bin El-Ouidane dam catchment area; source: own elaboration

on the slopes of high mountains and on the banks of the thalwegs, which sometimes form steep gorges carved out by rivers during the geological past of the region. Thus, this class of topographical factors is associated with steep slopes representing nearly 37% of the total surface area of the catchment area, with inclinations ranging from 20 to 75°. These areas are very vulnerable to the runoff.

The low values correspond to the plateaus e.g. El Houanet, the plateau of the lakes, Ait Abdi plateau, and the Ait Mhamed plateau, and the depressions and basins, such as the Ouaouizert basin, Tizi n'Isly, and Tagleft syncline. This slope ranges between 0 and 20° and represents 63% of the total surface area of the catchment area.

### LAND USE (C-FACTOR)

As shown in Figure 5, most of the upstream part of the catchment area does not benefit from any vegetation protection against erosion (bare soils in altitude). The densest forest covers, and therefore the most protective, are located at lower altitudes, in the thalweg of the rivers, where rainfall occurs most and temperatures stay at adequate levels.

As the soils are poorly developed, based on remote sensing, their surface characteristics are very close to those of their parent rocks. Thus, the present model may estimate soil losses in localities where the bedrock is already bare. This is particularly the case on summits, where the surface is also subject to wind erosion, freeze-thaw cycles (rock falls), and slopes too steep to retain the soil.

Besides, the persistent snow cover concerning the highest altitudes (see Fig. 3 or Fig. 4) constitutes protection against rainfall erosivity. Therefore, in these areas, the C-factor is lowered by considering a null value during four months of the year.

### RUSLE SOIL LOSSES ESTIMATION (A)

Evaluation, mapping, and the superposition of the different erosion factors (*R*, *K*, *LS*, *C*, *P*), carried out with the help of the GIS, resulted in the 30 m resolution soil loss map of the Bin El-Ouidane dam catchment area.

RUSLE yields an average erosion rate of 16.3 t·ha<sup>-1</sup>·y<sup>-1</sup> for an overall annual loss of 10.7 mln tonnes.

### DEPOSITION MODEL AND CORRECTED ESTIMATION

The unit stream power theory-based model estimates deposition over 32% of the catchment area. Once the deposition areas are excluded from the RUSLE calculation (Fig. 8), the model yields an average erosion rate of 10.3 t·ha<sup>-1</sup>·y<sup>-1</sup> and an overall annual loss of 6.73 mln t.

Moreover, the total deposition potential is estimated at 39% of the sediment transport capacity. Considering that this proportion of eroded particles is deposited before reaching the river system, the net mean erosion rate drops to 6.3 t·ha<sup>-1</sup>·y<sup>-1</sup> for an annual sediment production of 4.1 mln t. The last result is very consistent with the 5 mln m<sup>3</sup>·y<sup>-1</sup> siltation rate of the dam. Assuming characteristic values of superficial silts (Migniot, 1989) (density of 1.5 and siccidity of 50%), this siltation rate translates into a net erosion rate of 6.1 t·ha<sup>-1</sup>·y<sup>-1</sup>. The estimation is also consistent with previous studies, i.e. Fox *et al.* [1997] stated a mean erosion rate of 6.8 t·ha<sup>-1</sup>·y<sup>-1</sup> for the Bin El Ouidane catchment area.

The importance of combining RUSLE with a more physical approach to better account for the erosion/deposition phenomena was outlined by Manaouch *et al.* (2021). It is particularly important in the Moroccan context, where the models are often used outside their application range. A number of developments have been made concerning erosion/deposition models (Mitasova *et al.*, 2013), but the lack of calibrated parameters for the study context prevents a more refined estimate of deposition

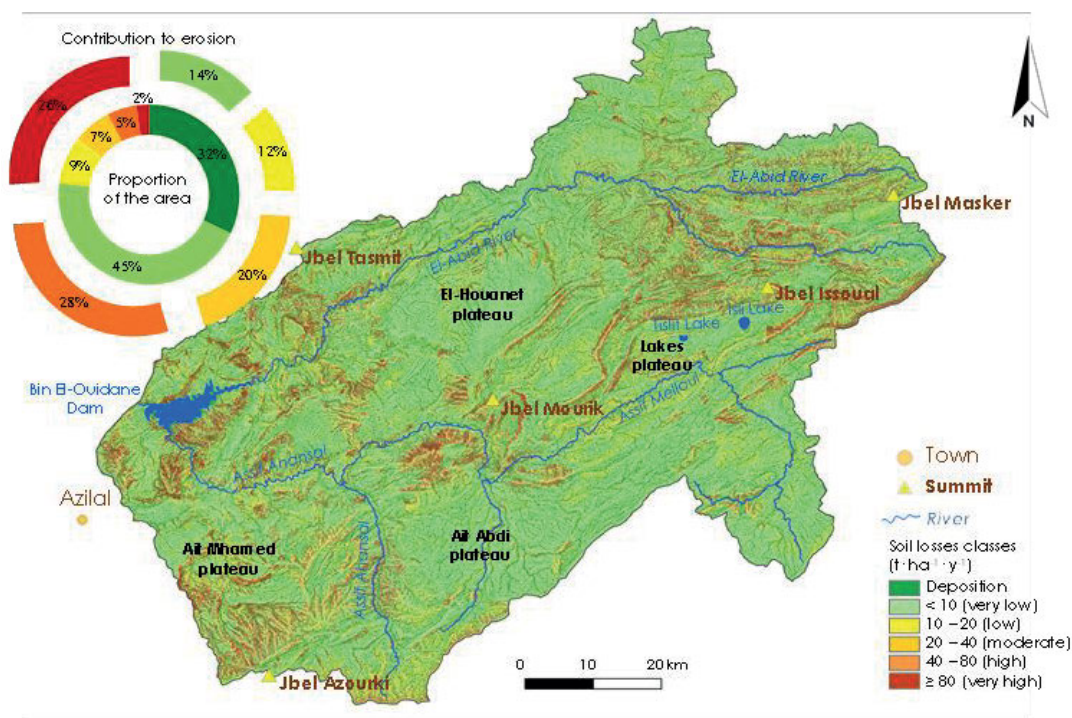


Fig. 8. Erosion and deposition estimation in the Bin El-Ouidane dam catchment area; source: own elaboration

rates at the pixel level. However, the correction made to RUSLE in our study at the basin scale is considered satisfactory, as the results match the data observed at the outlet.

The distribution of the erosion rates (Fig. 8) shows that most of the losses occur in a very small portion of the catchment. Indeed, the highest rates ( $>40 \text{ t}\cdot\text{ha}^{-1}\cdot\text{y}^{-1}$ ) account for 54% of the global loss, while they concern only 7% of the area. They are located on the steepest slopes (crest of mountain ranges and banks of thalwegs), even more so when the soil is left bare under unfavorable climatic and edaphic conditions. On the contrary, almost half of the catchment area undergoes very low erosion ( $<10 \text{ t}\cdot\text{ha}^{-1}\cdot\text{y}^{-1}$ ). In particular, the plateaus represent very low-risk areas, favored by a flat relief and high infiltration characteristic of karst formations (El Houanet karst, Jbel Chitou karst, Imghal karst, Ait Mazigh karst, and Ait Abdi karst). This type of distribution is typical of mountainous areas, as shown by Abaoui *et al.* (2005).

The deposition sites are spread over the whole area thanks to slope breaks that almost always appear in complex topographies, including in high mountains. The succession of erosion/deposition patterns and their representation through the model are illustrated in Figure 9. Zooming into the model results (Fig. 9a and Fig. 9b) shows the presence of depositional areas within complex slopes and a very good representation of the protective role of the forest cover compared to bare ground areas. The relevance of the deposition model can also be visualised through color shades of soil on a satellite image (Fig. 9c). Indeed, on the same hillside, the soil loses its organic matter and shows a lesser structure in eroded areas compared to deposition areas, hence a difference in color. The correspondence between the results and the field reality is made more visible by means of a juxtaposition in Figure 9d.

## LIMITATIONS AND PERSPECTIVES

Despite the adjunction of a deposition model to RUSLE, the results indicates erosion rates higher than sustainable soil loss, that ranges from 2 to  $12 \text{ t}\cdot\text{ha}^{-1}\cdot\text{y}^{-1}$  (Schertz, 1983). Moreover, the risk of biased estimation of erosion rates still exists due to methodological limitations. First, there is a lack of meteorological data in the area, both spatially and temporally. Comprehensive and seasonal knowledge of the climate in altitude would allow a better representation of the snow cycle (snowfall, snow cover, and snowmelt), which is critical in a high mountain environment (Schmidt *et al.*, 2018). On a similar point, the intra-annual variability of the RUSLE factors (mainly rainfall erosivity and vegetation cover) can follow asynchronous patterns that make the estimate biased via annual averages (Nouaim *et al.*, 2022). Second, the soil and geological setting of the region cause a high degree of uncertainty while determining the presence of soil, especially on bare sloping soils where the highest rates are finally estimated. Indeed, the stoniness (accounting notably for the outcrop of the bedrock) is an important correction to be made in order not to overestimate soil erosion (Panagos *et al.*, 2014).

## CONCLUSIONS

The water erosion in the Bin El-Ouidane dam catchment estimated thanks to RUSLE only yields an annual soil loss of 10.7 mln t and an average rate of  $16.4 \text{ t}\cdot\text{ha}^{-1}\cdot\text{y}^{-1}$ . The integration of the deposition phenomenon in the modeling using the unit stream power theory lowers the estimation to 4.1 mln t of annual losses and an average rate of  $6.3 \text{ t}\cdot\text{ha}^{-1}\cdot\text{y}^{-1}$ . These corrected results are very consistent with the siltation rate of the dam, which loses

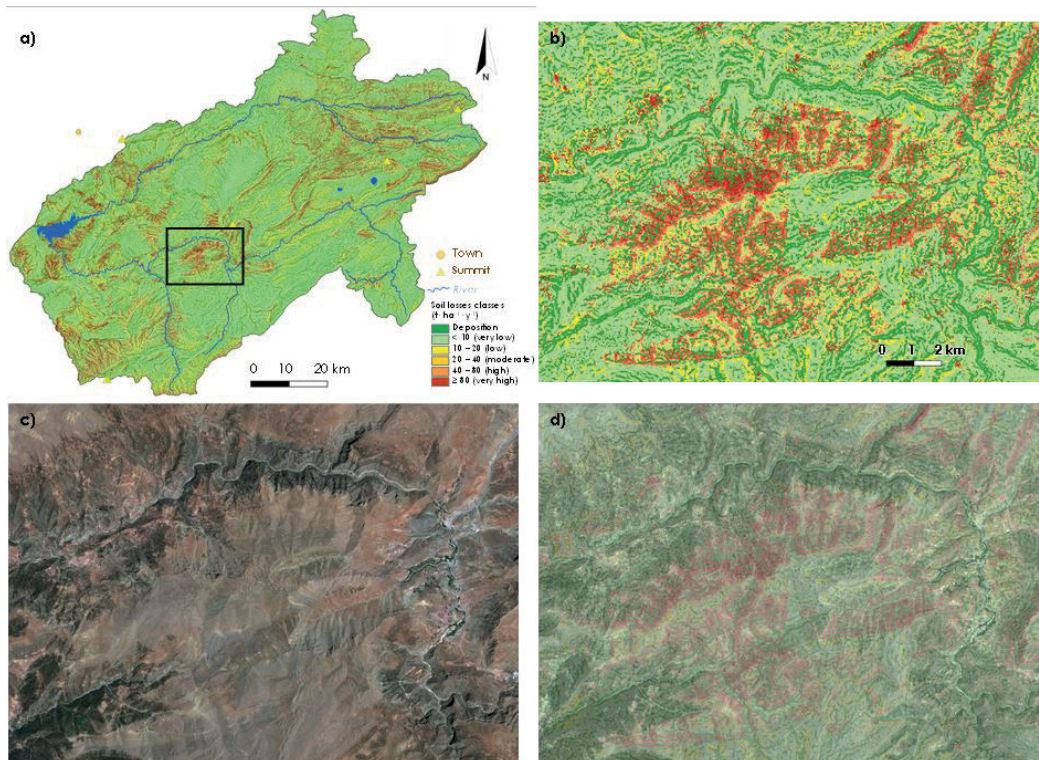


**Fig. 9.** Visual assessment of the method: a) position of the selected area in the catchment, b) modelled erosion, c) satellite image, d) superposition of the model and the satellite image; source: own elaboration

around 5 mln m<sup>3</sup> of water per year. The model also shows good agreement with the characteristics of the terrain visible via satellite images, which, in particular, indicates a pattern of erosion/deposition within the same hillslope.

The results of the present study prove the need to add a physical approach to the erosion/deposition phenomenon to the RUSLE model, which otherwise tends to greatly overestimate soil losses.

If some conservation programs define a soil loss tolerance ranging from 2 to 12 t·ha<sup>-1</sup>·y<sup>-1</sup>, these rates are always much higher than soil formation rates, especially in a semi-arid context. Moreover, some locations in the water catchment area are subject to very high erosion rates (more than 40 t·ha<sup>-1</sup>·y<sup>-1</sup>) because of very steep slopes and sparse vegetation cover. Therefore, soil conservation is a critical issue for the region as subsistence farming and pastoralism depend on the ability of the land to grow food and fodder. Also, the siltation of the dam threatens its functions (water storage for drinking water supply and irrigation in particular). In this context, the erosion map produced by this study gives the public authorities and other stakeholders (farmers) a tool to locate and prioritise the conservation programs (including mechanical erosion control techniques, reforestation, and overgrazing prevention).

Despite the correction made to RUSLE, the study still highlighted methodological issues, such as the lack of data (especially concerning rainfall and snow cover), but also modelling aspects (time discretisation to account for RUSLE parameters asynchronous yearly cycle or soil rockiness for example).

## REFERENCES

- Abaoui, J. *et al.* (2005) "Cartographie de l'érosion hydrique en zone montagneuse : cas du bassin versant des Ait Bou Goumez, Haut Atlas, Maroc [Mapping of water erosion in mountainous areas: case of the Ait Bou Goumez watershed, High Atlas, Morocco]," *Estudios Geológicos*, 61(1), pp. 33–39.
- Aboulabbès, O. (2004) *Etudes de diagnostic en hydrogéologie du SIBE de Tamga [Hydrogeological diagnostic of the Tamga's site of biological and environmental interest]*. Rabat: Haut Commissariat aux Eaux et Forêts et à la Lutte contre la Désertification.
- Al Zitawi, F. (2006) *Using RUSLE in prediction of soil loss for selected sites in North and North West of Jordan*. Irbid: Jordan University of Science and Technology.
- Arnoldus, H.M. (1980) "An approximation of the rainfall factor in the Universal Soil Loss Equation," in M. De Boodt, D. Gabriels (eds.) *Assessment of erosion*. Chichester: John Wiley and Sons, pp. 127–132.
- Badraoui, A. and Hajji, A. (2001) "Envasement des retenues de barrages [Siltation in dam basins]," *La Houille Blanche*, 87(6–7), pp. 72–75. Available at: <https://doi.org/10.1051/lhb/2001073>.
- Diallo, D. (2000) *Erosion des sols en zone soudanienne du Mali – Transfert des matériaux érodés dans le bassin versant de Djitiko (Haut Niger) [Soil erosion in the Sudanian zone of Mali – Transfer of eroded materials in the Djitiko watershed (Upper Niger)]*. Grenoble: Université Joseph Fourier.
- FAO (2015) *Status of the World's soil resources*. Rome: Foods and Agriculture Organization of the United Nations.
- Fox, H.R. *et al.* (1997) "Soil erosion and reservoir sedimentation in the High Atlas Mountains, southern Morocco," in D.E. Walling and J.-L. Probst (eds.) *Human impact on erosion and sedimentation, IAHS Publication*, 245, pp. 233–240.
- Geddes, N. and Dunkerley, D. (1999) "The influence of organic litter on the erosive effects of raindrops and of gravity drops released from desert shrubs," *Catena*, 36(4), pp. 303–313. Available at: [https://doi.org/10.1016/S0341-8162\(99\)00050-8](https://doi.org/10.1016/S0341-8162(99)00050-8).
- Gray, D. (2016) "Effect of slope shape on soil erosion," *Journal of Civil & Environmental Engineering*, 6(3), 231. Available at: <https://doi.org/10.4172/2165-784X.1000231>.
- Hara, F. *et al.* (2020) "Study of soil erosion risks using RUSLE model and remote sensing: case of the Bouregreg watershed (Morocco)," *Proceedings of IAHS*, 383, pp. 159–162. Available at: <https://doi.org/10.5194/piahs-383-159-2020>.
- Heusch, B. (1970) *L'érosion du pré-rif : une étude quantitative de l'érosion hydraulique dans les collines marneuses du pré-rif occidental [Pre-rif erosion: a quantitative study of hydraulic erosion in the marl hills of the western pre-rif]*. Rabat: Station de Recherches Forestières de Rabat.
- Julien, P.Y. (2010) *Erosion and sedimentation*. Cambridge: Cambridge University Press.
- Khemiri, K. and Jebari, S. (2021) "Evaluation de l'érosion hydrique dans les bassins versants de la zone semi-aride tunisienne avec les modèles RUSLE et MUSLE couplés à un système d'information géographique [Assessment of water erosion in the watersheds of the Tunisian semi-arid zone with the RUSLE and MUSLE models coupled to a GIS]," *Cahiers Agricultures*, 30, 7. Available at: <https://doi.org/10.1051/cagri/2020048>.
- Kouli, M., Souplos, P. and Vallianatos, F. (2008) "Soil erosion prediction using the Revised Universal Soil Loss Equation (RUSLE) in a GIS framework, Chania, Northwestern Crete, Greece," *Environmental Geology*, 57(3), pp. 483–497. Available at: <https://doi.org/10.1007/s00254-008-1318-9>.
- Le Bissonnais, Y. *et al.* (1998) "Crusting, runoff and sheet erosion on silty loamy soils at various scales and upscaling from m<sup>2</sup> to small catchments," *Soil & Tillage Research*, 46, pp. 69–80. Available at: [https://doi.org/10.1016/S0167-1987\(98\)80109-8](https://doi.org/10.1016/S0167-1987(98)80109-8).
- Lee, S., Wolberg, G. and Shin, S.Y. (1997) "Scattered data interpolation with multilevel B-splines," *IEEE Transactions on Visualization and Computer Graphics*, 3(3), pp. 228–244. Available at: <https://doi.org/10.1109/2945.620490>.
- Liu, B.Y. *et al.* (2000) "Slope length effects on soil loss for steep slopes," *Soil Science Society of American Journal*, 64(5), pp. 1759–1763. Available at: <https://doi.org/10.2136/sssaj2000.6451759x>.
- Liu, B.Y., Zhang, K. and Yun, X. (2002) "An empirical soil loss equation," *Proceedings of the 12<sup>th</sup> ISCO Conference*, 2, pp. 21–25.
- Ludwig, B. (2000) "Les déterminants agricoles du ruissellement et de l'érosion – De la parcelle au bassin versant [Agricultural determinants of runoff and erosion – From plot to watershed]," *Ingénieries*, 22, pp. 37–47.
- MAEF (2013) *Programme d'action nationale de lutte contre la désertification [National action programme to combat desertification]*. Rabat: Ministère de l'agriculture, du développement rural et des eaux et forêts.
- Maimouni, S. *et al.* (2011) "Potentiels et limites des indices spectraux pour caractériser la dégradation des sols en milieu semi-aride [Potential and limitations of spectral indices to characterise soil degradation in semi-arid environments]," *Canadian Journal of Remote Sensing*, 37(3), pp. 285–301. Available at: <https://doi.org/10.5589/m11-038>.
- Manaouch, M., Zouagui, A. and Fenjro, I. (2021) "A review of soil erosion modeling by RUSLE in Morocco: Achievements and limits," *E3S Web of Conferences*, 234, pp. 1–7. Available at: <https://doi.org/10.1051/e3sconf/202123400067>.

- Meliho, M. *et al.* (2016) "Cartographie des risques de l'érosion hydrique par l'équation universelle révisée des pertes en sols, la télédétection et les SIG dans le bassin versant de l'Ourika (Haut Atlas, Maroc) [Water erosion risk mapping using the revised universal soil loss equation, remote sensing and GIS in the Ourika watershed (High Atlas, Morocco)]," *European Scientific Journal*, 12(32), pp. 277–297. Available at: <https://doi.org/10.19044/esj.2016.v12n32p277>.
- Merzouki, T. (1992) "Diagnostic de l'envasement des grands barrages marocains [Diagnosis of silting in large Moroccan dams]," *Revue Marocaine du Génie Civil*, 38, pp. 46–50.
- Migniot, C. (1989) "Tassement et rhéologie des vases. Première partie [Bedding-down and rheology of muds]," *La Houille Blanche*, 75 (1), pp. 11–29. Available at: <https://doi.org/10.1051/lhb/1989001>.
- Millington, A.C. and Townshend, J.R. (1984) "Remote sensing applications in African erosion and sedimentation studies," *Proceedings of the IAHS Harare Symposium*, 144, pp. 373–384.
- Mitasova, H. *et al.* (1996) "Modelling topographic potential for erosion and deposition using GIS," *International Journal of Geographical Information Systems*, 10(5), pp. 629–641. Available at: <https://doi.org/10.1080/02693799608902101>.
- Mitasova, H. *et al.* (2013) "GIS-based soil erosion modelling," *Treatise on Geomorphology*, 3, pp. 228–258. Available at: <https://doi.org/10.1016/B978-0-12-374739-6.00052-X>.
- Moore, I.D. and Burch, G.J. (1986) "Modelling erosion and deposition: topographic effects," *Transactions of the American Society of Agricultural and Biological Engineers*, 29(6), pp. 1624–1630. Available at: <https://doi.org/10.13031/2013.30363>.
- Nashhaj, J. (2009) *Evaluation de l'érosion des sols et proposition d'aménagement du bassin versant à l'aval du barrage de Hassan II, Haute Moulouya, Maroc [Soil erosion assessment and watershed management proposal downstream of the Hassan II dam, Upper Moulouya, Morocco]*. Rabat: Institut Agronomique et Vétérinaire Hassan II.
- Nouaim, W. *et al.* (2022) "Assessing the intra-annual variability of agricultural soil losses: a RUSLE application in Nord-Pas-de-Calais, France," 52, pp. 210–220. Available at: <https://doi.org/10.24425/jwld.2022.140392>
- O'Loughlin, C. and Zhang, X.B. (1986) "The influence of fast-growing conifer plantations on shallow landsliding and earthflow movement in New Zealand steeplands," *IUFRO Yugoslavia*, 1, pp. 217–226.
- Pajot, G. (1963) *Etude des sols du Pré-Rif [Pre-Rif soil survey]*. Rabat: Institut National de Recherche Agricole.
- Panagos, P. *et al.* (2014) "Soil erodibility in Europe: A high-resolution dataset based on LUCAS," *Science of the Total Environment*, 479–480, pp. 189–200. Available at: <https://doi.org/10.1016/j.scitotenv.2014.02.010>
- Renard, K.G. *et al.* (1997) "Predicting soil erosion by water: A guide to conservation planning with the Revised Universal Soil Loss Equation (RUSLE)," *Agriculture Handbook*, 703. Tucson: U.S. Department of Agriculture.
- Roose, E. (1973) *Dix-sept années de mesures expérimentales de l'érosion et du ruissellement sur un sol ferrallitique sableux de basse Côte d'Ivoire : contribution à l'étude de l'érosion hydrique en milieu intertropical [17 years of experimental measurements of erosion and runoff on a ferrallitic sandy soil of the lower Ivory Coast: contribution to the study of water erosion in an intertropical environment]*. Abidjan: ORSTOM.
- Roose, E. and Bertrand, R. (1971) "Contribution à l'étude des méthodes des bandes d'arrêt pour lutter contre l'érosion hydrique en Afrique de l'Ouest : résultats expérimentaux et observations sur le terrain [Contribution to the study of stop strip methods for water erosion control in West Africa: experimental results and field observations]," *Agronomie Tropicale*, 26(11), pp. 1270–1283.
- Schertz, D. (1983) "The basis for soil loss tolerances," *Journal of Soil and Water Conservation*, 38, pp. 10–15.
- Schmidt, S., Alewell, C. and Meusburger, K. (2018) "Mapping spatiotemporal dynamics of the cover and management factor (C-factor) for grasslands in Switzerland," *Remote Sensing of Environment*, 211, pp. 89–104. Available at: <https://doi.org/10.1016/j.rse.2018.04.008>.
- Schmidt, S., Tresch, S. and Meusburger, K. (2019) "Modification of the RUSLE slope length and steepness factor (LS-factor) based on rainfall experiments at steep alpine grasslands," *MethodsX*, 6, pp. 219–229. Available at: <https://doi.org/10.1016/j.mex.2019.01.004>.
- Stone, R.P. and Hilborn, D. (2000) *Universal Soil Loss Equation: Factsheet*. Guelph: Ontario's Ministry of Agriculture, Food and Rural Affairs.
- Winchell, M.F. *et al.* (2008) "Extension and validation of a geographic information system-based method for calculating the revised universal soil loss equation length-slope factor for erosion risk assessments in large watersheds," *Journal of Soil and Water Conservation*, 63(3), pp. 105–111. Available at: <https://doi.org/10.2489/jswc.63.3.105>.
- Wischmeier, W.H. and Smith D.D. (1978) "Predicting rainfall erosion losses – A guide to conservation planning," *Agriculture Handbook*, 537. Washington, D.C.: U.S. Department of Agriculture.
- Wischmeier, W.H., Smith, D.D. and Uhland, R.E. (1958) "Evaluation of factors in the soil loss equation," *Agricultural Engineering*, 39, pp. 458–462.